Inorganica Chimica Acta 362 (2009) 1591–1599

Contents lists available at ScienceDirect

Inorganica Chimica Acta

journal homepage: www.elsevier.com/locate/ica

Synthesis, crystal structures, DNA binding and cleavage activity of L-glutamine copper(II) complexes of heterocyclic bases

Ashis K. Patra, Sovan Roy, Akhil R. Chakravarty *

Department of Inorganic and Physical Chemistry, Indian Institute of Science, Sir C.V. Raman Avenue, Bangalore 560 012, India

ARTICLE INFO

Article history:
Received 17 March 2008
Accepted 7 August 2008
Available online 15 August 2008

Keywords:
Copper(II) complex
L-Glutamine
Heterocyclic base
Crystal structure
DNA binding
DNA photocleavage

ABSTRACT

Ternary L-glutamine (L-gln) copper(II) complexes [Cu(L-gln)(B)(H_2O)](X) (B = 2,2′-bipyridine (bpy), X = $0.5SO_4^{2-}$, **1**; B = 1,10-phenanthroline (phen), X = ClO_4^-, **2**) and [Cu(L-gln)(dpq)(ClO_4)] (**3**) (dpq, dipyridoquinoxaline) are prepared and characterized by physicochemical methods. The DNA binding and cleavage activity of the complexes have been studied. Complexes **1–3** are structurally characterized by X-ray crystallography. The complexes show distorted square pyramidal (4+1) CuN_3O_2 coordination geometry in which the N,O-donor amino acid and the N,N-donor heterocyclic base bind at the basal plane with a H_2O or perchlorate as the axial ligand. The crystal structures of the complexes exhibit chemically significant hydrogen bonding interactions besides showing coordination polymer formation. The complexes display a d–d electronic band in the range of 610–630 nm in aqueous-dimethylformamide (DMF) solution (9:1 v/v). The quasireversible cyclic voltammetric response observed near −0.1 V versus SCE in DMF–TBAP is assignable to the Cu(II)/Cu(I) couple. The binding affinity of the complexes to calf thymus (CT) DNA follows the order: **3** (dpq) > **2** (phen) ≫ **1** (bpy). Complexes **2** and **3** show DNA cleavage activity in dark in the presence of 3-mercaptopropionic acid (MPA) as a reducing agent *via* a mechanistic pathway forming hydroxyl radical as the reactive species. The dpq complex **3** shows efficient photo-induced DNA cleavage activity on irradiation with a monochromatic UV light of 365 nm in absence of any external reagent. The cleavage efficiency of the DNA minor groove binding complexes follows the order: **3** > **2** ≫ **1**. The dpq complex exhibits photocleavage of DNA on irradiation with visible light of 647.1 nm. Mechanistic data on the photo-induced DNA cleavage reactions reveal the involvement of singlet oxygen ($^1O_2$) as the reactive species in a type-II pathway.

1. Introduction

Transition metal complexes with their efficient DNA binding and cleavage properties under physiological conditions have found wide applications in nucleic acids chemistry [1–15]. The use of such complexes in footprinting studies, as sequence specific DNA binding agents, as diagnostic agents in medicinal applications and for genomic research has generated current interests to develop this chemistry further. The DNA cleavage reactions are generally targeted towards different constituents of DNA, viz. the heterocyclic bases, deoxyribose sugar moiety and phosphodiester linkage. The oxidative DNA cleavage involves in the nucleobase oxidation and/or degradation of the sugar moiety by abstraction of sugar hydrogen atom(s), while the hydrolytic cleavage of DNA takes place due to hydrolysis of the phosphodiester bond. Among different modes of DNA cleavage, oxidative cleavage of DNA on irradiation with visible light is of our interest for potential applications of such compounds in the chemistry of photodynamic therapy (PDT) of cancer [16–25].

Porphyrin and phthalocyanine-based organic dyes are known to cause oxidative cleavage of DNA on photo-irradiation in red light [16–18]. Such compounds are used as potential drugs in PDT [16]. Photofrin®, the FDA approved PDT drug, is a hematoporphyrin species. Transition metal complexes showing light-induced DNA cleavage activity are primarily limited to the ruthenium and rhodium complexes of polypyridyl bases for their known photophysical properties [21–25]. Recently, a platinum(IV) complex as a potential *cis*-platin alternative is reported to show photo-cytotoxic activity [26]. The chemistry of 3d-metal complexes showing DNA photocleavage activity in visible light is less explored [27–33]. We are interested to study the DNA binding and photo-induced DNA cleavage activity of bio-essential α-amino acid copper(II) complexes. Our recent reports have shown that ternary copper(II) complexes of the type "A-Cu-B", where the amino acid like L-methionine, L-lysine or L-arginine (A) and heterocyclic DNA-binding phenanthroline bases (B) are covalently linked to the metal ion, show efficient red light-induced DNA cleavage activity in the PDT window of 600–800 nm [34–38]. In contrast, organic conjugates

* Corresponding author. Tel.: +91 80 22932533; fax: +91 80 23601552.
E-mail address: arc@ipc.iisc.ernet.in (A.R. Chakravarty).

0020-1693/$ - see front matter © 2008 Elsevier B.V. All rights reserved.
doi:10.1016/j.ica.2008.08.003

of the type "A–B" in which an amino acid moiety (A) is covalently linked to a photoactive DNA intercalator (B) are known to show DNA cleavage activity only in UV light [39–41].

The present work stems from our interests to develop this chemistry further by synthesizing new ternary copper(II) complexes of α-amino acid L-glutamine and N,N-donor heterocyclic bases. This amino acid with its terminal –C(=O)–NH_2 group has the potential to form significant hydrogen bonding interactions with the double-stranded (ds) DNA and could show good DNA-binding propensity. Herein we report the synthesis, crystal structures, DNA-binding and oxidative DNA cleavage activity of ternary L-glutamine (L-gln) copper(II) complexes [Cu(L-gln)(B)(H_2O)](X) (B = 2,2′-bipyridine (bpy), X = $0.5SO_4^{2-}$, **1**; B = 1,10-phenanthroline (phen), X = ClO_4^-, **2**) and [Cu(L-gln)(dpq)(ClO_4)] (**3**) (dpq, dipyridoquinoxaline) (Scheme 1). The significant result of this study is the metal-assisted red light-induced DNA cleavage activity of complex **3**.

2. Experimental

2.1. Materials

The reagents and chemicals of analytical grade were procured from commercial sources. Solvents used for electrochemical and spectroscopic studies were purified by standard procedures [42]. Supercoiled pUC19 (CsCl purified) DNA was purchased from Bangalore Genei (India). Agarose (molecular biology grade), distamycin, catalase, superoxide dismutase (SOD), ethidium bromide (EB) and calf thymus (CT) DNA were purchased from Sigma (USA). Tris–HCl buffer solution was prepared using deionized and sonicated triple distilled water. Dipyrido[3,2-*d*:2′,3′-*f*]quinoxaline (dpq) was prepared following a literature procedure [43].

2.2. General methods

Elemental analyses were done using a Thermo Finnigan Flash EA 1112 CHNSO analyzer. Infrared, absorption and fluorescence spectra were recorded on Perkin–Elmer Lambda 35, Perkin–Elmer Spectrum one 55 and Perkin–Elmer LS 50B spectrophotometers, respectively. Molar conductivity measurements were performed using a Control Dynamics (India) conductivity meter. Room temperature magnetic susceptibility data were obtained from a George Associates Inc. Lewis-coil force magnetometer using Hg[Co(NCS)$_4$] as a standard. Experimental susceptibility data were corrected for diamagnetic contributions [44]. Cyclic voltammetric measurements were made at 25 °C on a EG&G PAR Model 253 VersaStat potentiostat/galvanostat with electrochemical analysis software 270 using a three electrode set-up comprising of a glassy carbon working, platinum wire auxiliary and a saturated calomel reference (SCE) electrode. Tetrabutylammonium perchlorate (TBAP, 0.1 M) was used as a supporting electrolyte in DMF. The electrochemical data were uncorrected for junction potentials.

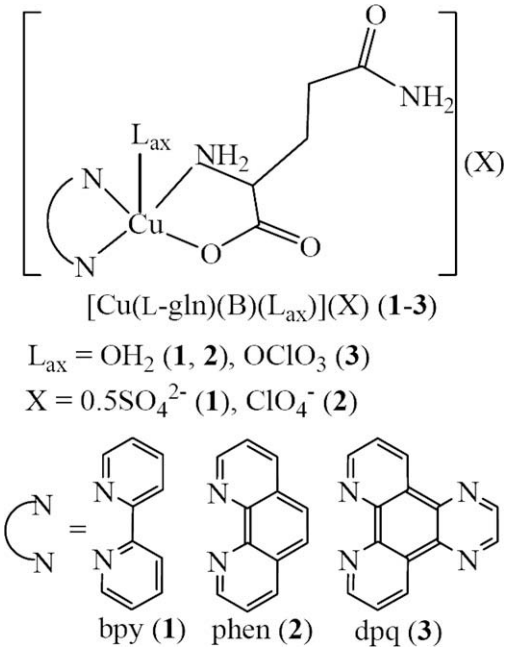

Scheme 1. Complexes **1**–**3** and the heterocyclic bases.

2.3. Synthesis of [Cu(L-gln)(B)(H_2O)](X) (B = bpy, X = $0.5SO_4^{2-}$, **1**; B = phen, X = ClO_4^-, **2**) and [Cu(L-gln)(dpq)(ClO_4)] (**3**)

The complexes were prepared by a general synthetic method in which an aqueous solution of $CuSO_4 \cdot 5H_2O$ (0.25 g, 1.0 mmol for **1**) or $Cu(ClO_4)_2 \cdot 6H_2O$ (0.37 g, 1.0 mmol for **2**, **3**) was initially reacted with an aqueous solution of L-glutamine (0.16 g, 1.1 mmol) treated with NaOH (0.040 g, 1.0 mmol), followed by slow addition of a methanol solution of the heterocyclic base [0.15 g, bpy, **1**; 0.18 g, phen, **2**; 0.22 g, dpq, **3** (0.9 mmol)]. The reaction mixture was stirred at 40 °C for 2 h and filtered. The filtrate on slow evaporation gave single crystals suitable for X-ray diffraction. The crystals were isolated and washed with aqueous methanol (1:1 v/v) before drying over P_4O_{10} (Yield: ~85%). For **1**, $C_{15}H_{19}CuN_4O_6S_{0.5}$: C, 41.78; H, 4.45; N, 13.01. Found: C, 41.47; H, 4.25; N, 13.12%. IR (KBr phase): 3363br, 3202br, 1658s, 1622s, 1497m, 1476m, 1445m, 1396m (SO_4^{2-}), 1319m, 1124s, 774m, 731m, 617m, 468w, 417w cm^{-1} (br, broad; w, weak; m, medium, s, strong; vs, very strong). Electronic spectrum in water [λ/nm (ε/M^{-1} cm^{-1})]: 237 (7950), 300 (8970), 310 (8250), 610 (50). Λ_M/S m^2 M^{-1} (in water, 25 °C) = 95. μ_{eff} (298 K): 1.78 μ_B. For **2**, $C_{17}H_{19}ClCuN_6O_7$: C, 42.23; H, 3.17; N, 15.55. Found: C, 42.17; H, 3.05; N, 15.42%. IR (KBr phase): 3525br, 3391br, 3070m, 1626m, 1608m, 1584s, 1555s, 1518m, 1446m, 1428s, 1340m, 1224m, 1147s, 1116s, 1088vs (ClO_4^-), 928m, 873m, 852s, 780w, 740m, 722s, 649w, 624s, 567w, 494m, 468m, 429w cm^{-1}. Electronic spectrum in H_2O [λ/nm (ε/M^{-1} cm^{-1})]: 273 (18060), 294 (5470), 622 (40). Λ_M/S m^2 M^{-1} (in H_2O, 25 °C) = 110. μ_{eff} (298 K): 1.74 μ_B. For **3**, $C_{19}H_{17}ClCuN_4O_8$: C, 40.32; H, 3.78; N, 11.06. Found: C, 40.17; H, 3.55; N, 10.94%. IR (KBr phase): 3697br, 3451br, 3296br, 3205br, 3054br, 1680s, 1643s, 1579m, 1486m, 1448w, 1409s, 1389s, 1339s, 1280w, 1230m, 1137s, 1083vs (ClO_4^-), 1060s (ClO_4^-), 1052s (ClO_4^-), 929m, 855m, 835s, 813m, 780m, 733s, 668m, 622s, 570s, 432m cm^{-1}. Electronic spectrum in H_2O [λ/nm (ε/M^{-1} cm^{-1})]: 258 (18500), 336 (1600), 628 (70). Λ_M/S m^2 M^{-1} (in H_2O, 25 °C) = 85. μ_{eff} (298 K): 1.72 μ_B.

2.4. Solubility and stability

The complexes showed good solubility in DMF, DMSO and water, less solubility in methanol and ethanol, and insolubility in hydrocarbons. They were found to be stable in the solid as well as in the solution phases. *Caution*! Perchlorate salts being potentially explosive, only small quantity was handled with care.

2.5. X-ray crystallographic procedures

The crystal structures of [Cu(L-gln)(bpy)(H_2O)]$(SO_4)_{1/2}$ (**1**), [Cu(L-gln)(phen)(H_2O)](ClO_4) (**2**) and [Cu(L-gln)(dpq)(ClO_4)] (**3**) were obtained by single crystal X-ray diffraction technique. Crystal mounting was done on glass fibers with epoxy cement. All geometric and intensity data were collected at room temperature using an

automated Bruker SMART APEX CCD diffractometer equipped with a fine focus 1.75 kW sealed tube Mo-Kα X-ray source (λ = 0.71073 Å) with increasing ω (width of 0.3° per frame) at a scan speed of 5, 4 and 8 s per frame for complexes **1–3**, respectively. The SMART software was used for data acquisition and the SAINT software for data extraction. Intensity data, collected using ω–2θ scan mode, were corrected for Lorentz-polarization effects and for absorption [45]. The structures were solved by the combination of Patterson and Fourier techniques and refined by full-matrix least-squares method using SHELX system of programs [46]. All hydrogen atoms belonging to the complex other than the aqua ligand were in their calculated positions and were refined using a riding model. All non-hydrogen atoms were refined anisotropically. Perspective views of the molecules were obtained by ORTEP [47]. Selected crystallographic data are summarized in Table 1.

2.6. DNA binding and cleavage experiments

The experiments involving the interaction of the ternary copper(II) complexes with CT and plasmid supercoiled (SC) DNA were carried out in Tris–HCl buffer (50 mM Tris–HCl, pH 7.2) at room temperature. Thermal denaturation studies were carried out in melting-buffer (5 mM Na_2HPO_4, 5 mM NaH_2PO_4, 1 mM Na_2EDTA and 5 mM NaCl). The buffer solution of calf thymus DNA gave a ratio of UV absorbance at 260 and 280 nm of about 1.89:1, indicating the DNA sufficiently free from protein [48]. The DNA concentration per nucleotide was measured from the absorption spectral band at 260 nm using the molar absorption coefficient (ε) of 6600 M^{-1} cm^{-1} [49].

2.6.1. Absorption spectroscopic studies

Absorption titration experiments were done using a complex concentration of 40 μM while varying the concentration of the CT DNA. An equal quantity of CT DNA was added to both the complex and the reference solutions to eliminate the absorbance of DNA itself. From the absorption data, the intrinsic binding constant K_b along with binding site size (s) were determined by regression analysis using Eq. (1):

$$(\varepsilon_a - \varepsilon_f)/(\varepsilon_b - \varepsilon_f) = (b - (b^2 - 2K_b^2 C_t[DNA]/s)^{1/2})/2K_b C_t, \quad (1)$$

$b = 1 + K_b C_t + K_b[DNA]/2s$, where ε_a is the extinction coefficient of the charge transfer band at a given DNA concentration, ε_f is the extinction coefficient of the complex free in solution, ε_b is the extinction coefficient of the complex when fully bound to DNA, K_b is the equilibrium binding constant, C_t is the total metal complex concentration, [DNA] is the DNA concentration in nucleotides and s is the binding site size in base pairs [50,51]. The calculation was done assuming non-cooperative metallointercalator binding of the complexes to DNA.

2.6.2. Fluorescence binding study

The relative binding of the ternary complexes to CT DNA was studied by fluorescence spectral method using ethidium bromide (EB) bound CT DNA solution in Tris–HCl/NaCl buffer (pH, 7.2). EB was non-emissive in Tris-buffer medium due to fluorescence quenching by the solvent molecules [52,53]. In the presence of CT DNA, it showed enhanced emission intensity due to intercalative binding to DNA. A competitive binding of the copper complexes to CT DNA resulted in the reduction of the emission intensity due to displacement of bound EB and/or quenching of the fluorescence of EB by paramagnetic copper(II) species. In a typical experiment, a 25 μL of CT-DNA solution (A_{260} = 2.0) was added to a 2.0 mL of EB buffer solution (pH 7.2) and the fluorescence intensity was measured using excitation wavelength of 546 nm resulting an emission at 600 nm at room temperature. Aliquots of 1.0 mM complex solution were then added to the EB bound DNA solution. The fluorescence intensity was measured after each addition until a 50% reduction of the intensity had occurred. The apparent binding constant (K_{app}) was calculated from the equation: $K_{EB} \times [EB] = K_{app} \times [complex]$, where [complex] is the concentration of the ternary complex at 50% reduction of fluorescence intensity [$K_{EB} = 1.0 \times 10^7$ M^{-1}, [EB] = 1.3 μM] [54].

2.6.3. Thermal denaturation studies

DNA melting experiments were carried out by monitoring the absorption intensity of CT DNA at 260 nm at various temperatures, both in the absence and presence of the ternary copper(II) complexes. Measurements were made using a Perkin–Elmer Lambda 35 spectrophotometer equipped with a Peltier temperature-controlling programmer (PTP 6, ±0.1 °C). The absorbance at 260 nm

Table 1
Selected crystallographic data for **1–3**

	1	**2**	**3**
Formula	$C_{15}H_{23}CuN_4O_{7.5}S_{0.5}$	$C_{17}H_{19}ClCuN_4O_8$	$C_{19}H_{17}ClCuN_6O_7$
Fw (g M^{-1})	458.94	506.35	540.38
Crystal system	monoclinic	monoclinic	triclinic
Space group (no.)	*C*2 (5)	$P2_1$ (4)	*P*1 (1)
a (Å)	25.807(8)	12.617(2)	8.746(2)
b (Å)	6.959(2)	5.3522(9)	9.416(2)
c (Å)	23.104(7)	14.811(2)	12.931(3)
α (°)	90.00	90.00	97.418(4)
β (°)	112.128(5)	91.024(3)	91.154(4)
γ (°)	90.00	90.00	98.364(4)
V (Å^3)	3844(2)	1000.0(3)	1043.9(5)
Z	8	2	2
T (K)	293(2)	293(2)	293(2)
ρ_{calc} (g cm^{-3})	1.586	1.682	1.719
λ (Å) (Mo Kα)	0.71073	0.71073	0.71073
μ (mm^{-1})	1.239	1.281	1.232
Data/restraints/parameter	7388/1/506	3368/1/356	9262/3/613
Goodness-of-fit on F^2	1.039	1.049	1.018
R (F_o)[a] ($I > 2\sigma(I)$) [R all data]	0.0490 [0.0644]	0.0281 [0.0305]	0.0395 [0.0483]
wR (F_o)[b] ($I > 2\sigma(I)$) [wR all data]	0.1135 [0.1237]	0.0680 [0.0693]	0.1009 [0.1068]
Largest difference in peak and hole (e Å^{-3})	0.849, −0.289	0.325, −0.221	0.921, −0.289
$W = 1/[\sigma^2(F_o^2) + (AP)^2 + (BP)]$	A = 0.0634; B = 0.0	A = 0.0380, B = 0.0	A = 0.0665; B = 0.0

[a] $R = \Sigma||F_o| - |F_c||/\Sigma|F_o|$.
[b] $wR = \sum[w(F_o^2 - F_c^2)^2]/\sum[w(F_o)^2]^{1/2}$; $w = [\sigma^2(F_o)^2 + (AP)^2 + BP]^{-1}$, where $P = (F_o^2 + 2F_c^2)/3$.

was continuously monitored for solutions of CT-DNA (160 μM) in the absence and presence of the copper(II) complex (15 μM) on increasing the temperature of the solution by 0.25 °C per min.

2.6.4. Viscosity measurement

Viscometric studies were done using a Schott Gerate AVS 310 Automated Viscometer that was thermostated at 37 °C in a constant temperature bath. The concentration of DNA was 100 μM in NP and the flow times were measured with an automated timer. Each sample was measured 3 times. An average flow time was calculated. The data were presented as $(\eta/\eta_0)^{1/3}$ versus [complex]/[DNA], where η is the viscosity of DNA in the presence of the complex and η_0 is that of DNA alone. Viscosity values were calculated from the observed flowing time of DNA-containing solutions (t) corrected for that of the buffer alone (t_0): $\eta = (t - t_0)$.

2.6.5. DNA cleavage study

The cleavage of supercoiled pUC19 DNA (30 μM, 0.2 μg, 2686 base-pair) by the complexes was studied by agarose gel electrophoresis in 50 mM Tris–HCl buffer (pH 7.2) containing 50 mM NaCl in the presence or absence of reducing agent under dark or illuminated conditions. For photo-induced DNA cleavage studies, the solutions were photo-exposed to UV light of 365 nm (12 W) or visible laser light of 647.1 nm using Spectra Physics Water-Cooled Mixed-Gas Ion Laser Stabilite® 2018-RM (beam diameter at $1/e^2$ = 1.8 mm ± 10% and beam divergence with full angle = 0.70 mrad ± 10%). The laser power at 647.1 nm was 100 mW, measured using Spectra Physics CW Laser Power Meter (Model 407A). After exposure to the light, each sample was incubated for 1.0 h at 37 °C and analyzed for the photo-cleaved products using gel electrophoresis as discussed below.

The inhibition reactions for the "chemical nuclease" reactions were carried out under dark conditions in the presence of reagents like distamycin (50 μM) and DMSO (4 μL) prior to the addition of the ternary complex and the reducing agent 3-mercaptopropionic acid (MPA). The inhibition reactions for the photo-induced DNA cleavage study were carried out at 365 nm using reagents, viz. NaN_3, 100 μM; DMSO, 4 μL; catalase, 4 units, prior to the addition of the complex. For the D_2O experiment, this solvent was used for dilution of the sample to 20 μL. The samples after incubation for 1.0 h at 37 °C in a dark chamber were added to the loading buffer containing 25% bromophenol blue, 0.25% xylene cyanol, 30% glycerol (3 μL) and the solution was finally loaded on 0.8% agarose gel containing 1.0 μg/mL ethidium bromide. Electrophoresis was carried out in a dark chamber for 3.0 h at 40 V in TAE (Tris–acetate EDTA) buffer. Bands were visualized by UV light and photographed. The extent of DNA cleavage was measured from the band intensities using UVITEC Gel Documentation System. Due corrections were made for the presence of low level of nicked circular (NC) form in the original supercoiled (SC) DNA sample and for the low affinity of EB binding to SC compared to NC and linear forms of DNA [55]. The concentrations of the complexes or the additives corresponded to the quantity of the sample after dilution to the 20 μL final volume with Tris–HCl buffer. The observed error in measuring the band intensities ranged between 3% and 7%.

3. Results and discussion

3.1. Synthesis and general aspects

Ternary L-glutamine copper(II) complexes containing heterocyclic bases are prepared in high yield from a general reaction in which a copper(II) salt is reacted with the N,N-donor heterocyclic base, viz. bpy, phen and dpq and the monoanionic amino acid. The complexes are formulated as $[Cu(L\text{-gln})(B)(L_{ax})](X)$ (**1–3**), where B is the bidentate heterocyclic base (bpy, phen, dpq), L_{ax} = axial ligand (H_2O or ClO_4^-) and X is SO_4^{2-} or ClO_4^- (Scheme 1). Selected physicochemical data are given in Table 2. The one-electron paramagnetic ($\mu_{eff} \sim 1.8\ \mu_B$) complexes show a d–d band near 600 nm in water (Fig. 1). The electronic bands observed near 300 nm are assignable to the intraligand transitions. The complexes are redox-active and show a quasireversible cyclic voltammetric response near 0.1 V versus SCE assignable to the Cu(II)/Cu(I) couple in DMF–0.1 M TBAP. The conductivity data indicate 1:1 electrolytic nature of the complexes giving $[Cu(L\text{-gln})(B)(H_2O)]^+$ in solution. The axial perchlorate ligand in **3**, formulated from the crystal structure, seems to undergo substitution in water forming axial aqua adduct.

3.2. Crystal structures

Complexes **1–3** are structurally characterized by single-crystal X-ray diffraction technique. The ORTEP views of the complexes are shown in Figs. 2–4. Selected bond distances and angles are given in Tables 3 and 4. The ternary complex $[Cu(L\text{-gln})(bpy)(H_2O)_{1/2}](SO_4)_{1/2} \cdot 2H_2O$ crystallizes in the non-centrosymmetric C2 space group of the monoclinic crystal system having two molecules and one sulfate lattice anion in the asymmetric unit. The metal center shows a (4+1) square-pyramidal CuN_3O_2 coordination geometry with half of sulfate anion per formula unit of the complex. The copper is bonded to one bidentate bpy ligand and one bidentate L-gln and an axial oxygen atom from aqua/carboxylate

Table 2
Physicochemical data and DNA binding parameters for the ternary copper(II) complexes **1–3**

Complex	1	2	3
IR[a]: (ν/cm^{-1})	1396 (SO_4^-)	1088 (ClO_4^-)	1083, 1060, 1052 (ClO_4^-)
d–d band: λ_{max}/nm (ε/M^{-1} cm^{-1})[b]	610 (50)	622 (40)	628 (70)
CV: $E_{1/2}$/V (ΔE_p/mV)[c]	−0.08 (540)	−0.09 (440)	−0.06 (410)
Λ_M[d]/S m^2 M^{-1}	95	110	85
μ_{eff}[e]/μ_B	1.78	1.74	1.72
K_b[f]/M^{-1}		3.8×10^4 (0.6)	3.7×10^5 (0.7)
K_{app}[g]/M^{-1}		6.3×10^5	4.78×10^6
ΔT_m[h]/°C		2.0	2.7

[a] KBr phase.
[b] In aqueous medium.
[c] Cu(II)/Cu(I) couple in DMF–0.1 M TBAP. $E_{1/2} = 0.5(E_{pa} + E_{pc})$, $\Delta E_p = |E_{pa} - E_{pc}|$, where E_{pa} and E_{pc} are the anodic and cathodic peak potentials, respectively. Scan rate: 50 mV s^{-1}.
[d] In aqueous medium at 25 °C.
[e] μ_{eff} for solid samples at 298 K.
[f] Intrinsic DNA binding constant (K_b) from absorption spectral method.
[g] Apparent DNA binding constant from competitive binding assay by emission method.
[h] Changes in melting temperature of CT DNA.

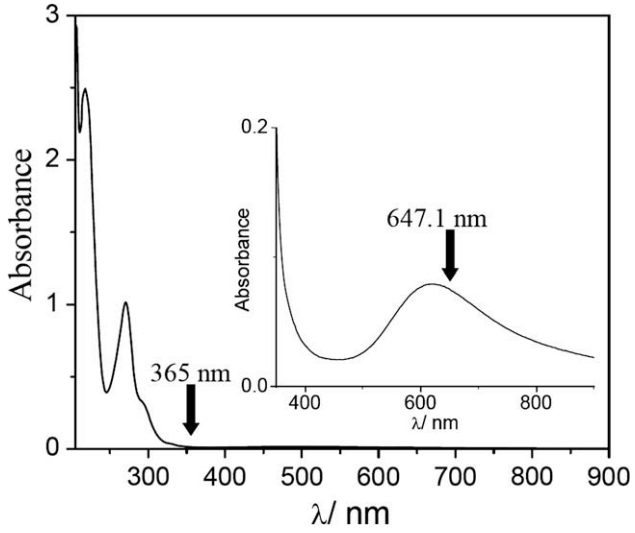

Fig. 1. Electronic spectra of [Cu(L-gln)(phen)(H_2O)](ClO_4) (**2**) in water. The inset shows the d–d band of the complex.

ligand. The pendant –$CONH_2$ group of the amino acid does not show any interaction with the metal ion. The average trigonal distortion parameter (τ) value is 0.04 [56]. The crystal structure displays the formation of a 1D coordination polymer in which one molecule having an aqua ligand at the axial position is linked at the other axial position to an oxygen atom of the carboxyl group belonging to another molecule giving (4+2) CuN_3O_3 coordination geometry. The structural features resemble well with the reported crystal structure of an analogous SMe-L-cys complex of copper(II) having dipyridophenazine base [37]. The 3D lattice structure shows the presence of extensive intermolecular non-covalent interactions involving the axial aqua ligand, lattice sulfate anion, lattice water molecules and L-gln. The hydrogen atom of the axial aqua ligand is hydrogen bonded (2.78 Å) to the carboxylate oxygen atom of another molecule. The hydrogen atoms of terminal NH_2 group of the pendant carboxamide group form hydrogen bond with the oxygen atom of the terminal –$CONH_2$ group of another molecule (distance ~ 2.91 Å). The sulfate oxygen atoms are also involved in the hydrogen bonding interactions with the amine hydrogen atoms and the terminal carboxamide group (distance ~ 2.96 Å).

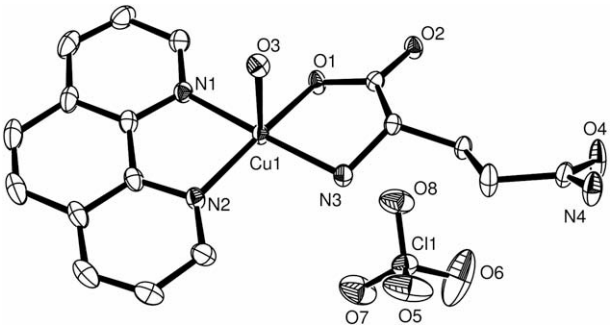

Fig. 3. ORTEP diagram of complex **2** showing 50% probability thermal ellipsoids with atom labeling scheme for the metal and heteroatoms.

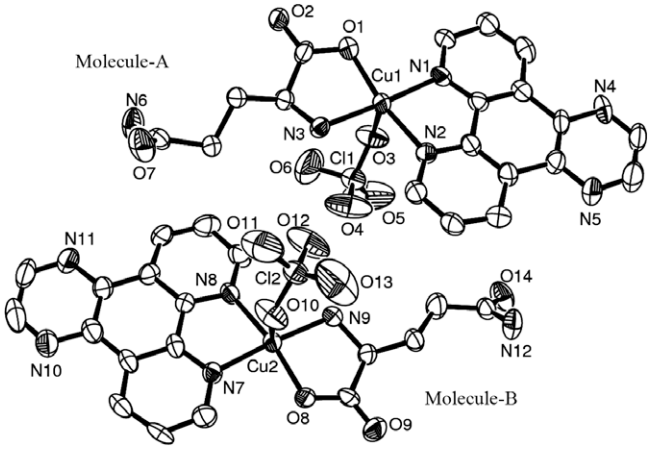

Fig. 4. ORTEP diagram of two independent molecules of complex **3** showing 50% probability thermal ellipsoids with atom labeling scheme for the metal and heteroatoms.

Complex **2** crystallizes in the monoclinic space group $P2_1$ with two molecules in the unit cell. The crystal structure of [Cu(L-gln)(phen)(H_2O)](ClO_4) (**2**) consists of an independent monomeric cationic complex containing bidentate N,O-donor L-glutamine and bidentate chelating N,N-donor phenanthroline in a square-pyramidal (4+1) coordination geometry with an aqua ligand at elongated

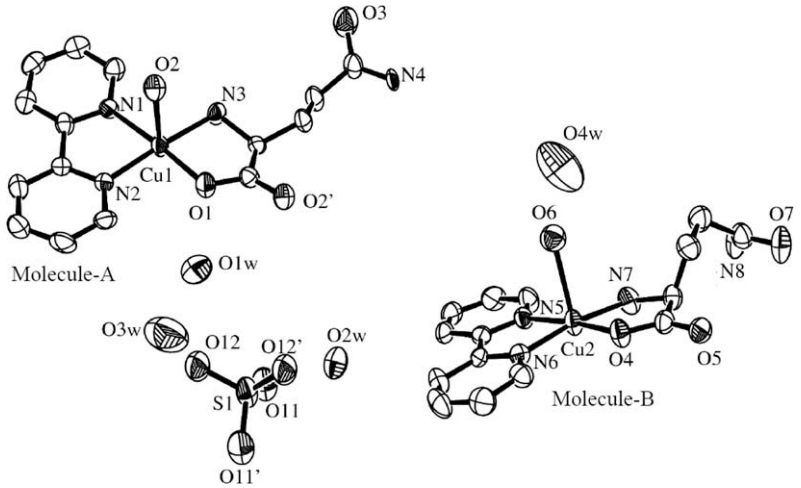

Fig. 2. ORTEP diagram of two molecules of complex **1** showing 50% probability thermal ellipsoids with atom labeling scheme for the metal and heteroatoms (symmetry transformation for O2′: 1/2 − *x*, −1/2 + *y*, 1 − *z*; O11′: 1 − *x*, *y*, 1 − *z* and O12′: 1 − *x*, *y*, 1 − *z*).

axial site. The trigonal distortion parameter (τ) value is 0.14. The Cu–O(L-gln), Cu–N(L-gln), Cu–N(phen) and Cu–O(H_2O) distances are 1.953(2), 1.995(3), 2.009(3) and 2.278(2) Å, respectively. The side alkyl chain of L-gln containing carboxamide group is a pendant moiety. The structure shows the presence of extensive intermolecular hydrogen bonding interactions. The hydrogen atoms of the axial aqua ligand are hydrogen bonded with the carboxylic oxygen atoms belonging to two other molecules (distance ~ 2.8 Å). One of the perchlorate oxygen atom forms hydrogen bond with the hydrogen atom of the NH_2 group bound to copper(II) (distance ~ 3.0 Å). Hydrogen atoms of the terminal NH_2 group of the carboxamide group form hydrogen bond with the oxygen atom of –$CONH_2$ belonging to another molecule (distance ~ 2.88 Å).

The ternary complex [Cu(L-gln)(dpq)(ClO_4)] (**3**) crystallizes in the non-centrosymmetric *P*1 space group of triclinic crystal system having two independent molecules in the crystallographic asymmetric unit (unit cell). The complex shows the copper(II) center bound to a bidentate N,O-donor L-gln with pendant carboxamide group, a bidentate chelating N,N-donor diypridoquinoxaline (dpq) and an axially bound perchlorate ligand in a square-pyramidal (4+1) geometry. The trigonal distortion parameter (τ) value is 0.14. The average Cu–O(L-gln), Cu–N(L-gln), Cu–N(dpq) and Cu–O(ClO_4) distances are 1.909 (4), 1.981 (5), 2.008 (5) and 2.441 (5) Å, respectively. The crystal structure shows extensive hydrogen bonding network. The hydrogen atoms of the NH_2 group of the carboxamide moiety are involved in hydrogen bonding interactions with one perchlorate oxygen atom and a carboxyl oxygen atom from another molecule (distance ~ 2.9 Å). The oxygen atom of the pendant –$CONH_2$ group is hydrogen bonded to the hydrogen atom of the NH_2 group bound to copper(II) of another molecule (distance ~ 2.78 Å). The weakly bound perchlorate ion seems to undergo substitution with an aqua ligand in H_2O as evidenced from the 1:1 electrolytic nature of this complex in solution.

Table 3
Selected bond distances (Å) and angles (°) for [Cu(L-gln)(bpy)(H_2O)$_{1/2}$](SO_4)$_{1/2}$ · $2H_2O$ (**1** · $2H_2O$)

Molecule-A		Molecule-B	
Cu(1)–O(1)	1.942(3)	Cu(2)–O(4)	1.936(3)
Cu(1)–N(1)	1.989(4)	Cu(2)–N(5)	2.014(4)
Cu(1)–N(2)	1.987(3)	Cu(2)–N(6)	2.004(4)
Cu(1)–N(3)	1.989(3)	Cu(2)–N(7)	1.980(4)
O(1)–Cu(1)–N(1)	173.81(15)	O(4)–Cu(2)–N(5)	173.65(15)
O(1)–Cu(1)–N(2)	92.94(14)	O(4)–Cu(2)– N(6)	92.78(15)
O(1)–Cu(1)–N(3)	83.99(14)	O(4)–Cu(2)– N(7)	84.55(16)
N(1)–Cu(1)–N(2)	81.37(15)	N(5)–Cu(2)–N(7)	100.65(16)
N(1)–Cu(1)–N(3)	101.77(14)	N(5)–Cu(2)–N(6)	81.56(16)
N(2)–Cu(1)–N(3)	176.51(19)	N(6)–Cu(2)–N(7)	171.5(2)

Table 4
Selected bond distances (Å) and angles (°) for the complexes [Cu(L-gln)(phen)(H_2O)](ClO_4) (**2**) and [Cu(L-gln)(dpq)(ClO_4)] (**3**) with estimated standard deviations (esd) in their parentheses

	2	**3**		
		Molecule-A	Molecule-B	
Cu(1)–O(1)	1.953(2)	1.904(4)	Cu(2)–O(8)	1.914(4)
Cu(1)–O(3)	2.278(2)	2.426(4)	Cu(2)–O(10)	2.456(5)
Cu(1)–N(1)	2.008(3)	2.001(4)	Cu(2)–N(7)	1.993(5)
Cu(1)–N(2)	2.010(3)	2.040(5)	Cu(2)–N(8)	2.000(5)
Cu(1)–N(3)	1.995(3)	1.968(4)	Cu(2)–N(9)	1.994(5)
O(1)–Cu(1)–O(3)	95.80(10)	94.85(18)	O(8)–Cu(2)–O(10)	92.34(17)
O(1)–Cu(1)–N(1)	93.82(10)	91.88(19)	O(8)–Cu(2)–N(7)	89.85(18)
O(1)–Cu(1)–N(2)	167.12(10)	166.23(19)	O(8)–Cu(2)–N(8)	168.91(19)
O(1)–Cu(1)–N(3)	82.46(10)	84.48(18)	O(8)–Cu(2)–N(9)	86.45(18)
N(1)–Cu(1)–N(2)	82.35(11)	81.86(19)	N(7)–Cu(2)–N(8)	82.07(19)
N(1)–Cu(1)–O(3)	90.08(10)	88.02(17)	N(7)–Cu(2)–O(10)	83.99(17)
N(2)–Cu(1)–O(3)	96.50(10)	97.17(17)	N(8)–Cu(2)–O(10)	94.34(19)
N(3)–Cu(1)–O(3)	92.53(12)	91.02(18)	N(9)–Cu(2)–O(10)	97.80(17)
N(3)–Cu(1)–N(1)	175.66(13)	176.1(2)	N(7)–Cu(2)–N(9)	175.9(2)
N(3)–Cu(1)–N(2)	100.79(11)	101.96(18)	N(9)–Cu(2)–N(8)	101.37(19)

3.3. DNA binding properties

3.3.1. Electronic spectral studies

Absorption titration method is used to monitor the interaction of the copper(II) complexes **1–3** with CT DNA. In general, a complex bound to DNA through intercalation results in hypochromism and red shift (bathochromism) of the absorption band due to strong stacking interaction between the aromatic chromophore of the complex and the base pairs of DNA [57]. In order to compare the binding strength of the complexes with CT DNA, the intrinsic equilibrium DNA binding constants (K_b) along with the binding site size (s) of the complexes to DNA are determined by monitoring the change of the absorption intensity of the charge transfer spectral band of the ternary complexes with increasing concentration of CT DNA (Fig. 5) [51]. The observed order of the DNA binding propensity is **3** (L-gln-Cu^{II}-dpq) > **2** (L-gln-Cu^{II}-phen) ≫ **1** (L-gln-Cu^{II}-bpy) (Table 2). It shows that the DNA binding affinity of the complexes increases with an increase in the extended planarity of the heterocyclic bases. The high K_b value for the dpq complex in comparison to its phen analogue is possibly due to the presence of a planar quinoxaline ring in the dpq ligand facilitating groove binding/stacking with the base pairs. The bpy complex **1** in absence of any planar moiety does not show any apparent binding to CT DNA. The pendant terminal amide group of the amino acid in complex **1** does not show any significant influence on the DNA binding property of the complex.

Relative binding of the ternary complexes to CT DNA has been studied by fluorescence spectroscopy using EB bound CT DNA solution in Tris–HCl/NaCl buffer (pH, 7.2). The DNA binding propensity of the present complexes is measured from the reduction in the emission intensity of EB at different complex concentrations. The DNA binding order observed from this study shows similar trend as obtained from the UV–Vis spectral study (Table 2).

3.3.2. Thermal denaturation and viscosity measurement

Thermal behavior of DNA in the presence of metal complexes can give information about the interaction strength of the com-

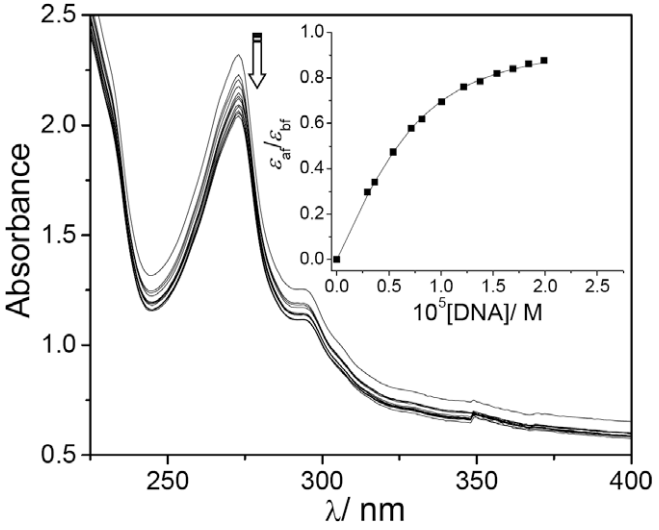

Fig. 5. Absorption spectral traces on addition of CT DNA to the solution of **2** (shown by arrow). Inset: plot of [DNA]/($\varepsilon_a - \varepsilon_f$) vs. [DNA] for absorption titration of CT-DNA with complex **2** (■).

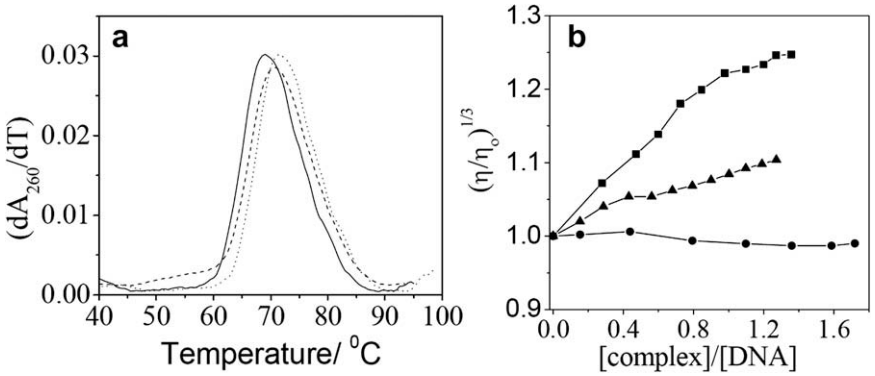

Fig. 6. (a) Effect of addition of complexes **2** (----) and **3** (···) (50 μM) on the melting temperature of CT- DNA (—) (200 μM) in 5 mM phosphate buffer (pH 6.85) with a ramp rate of 0.5 °C/min. (b) Change in relative specific viscosity of CT-DNA (150 μM) on addition of complexes **1** (●), **2** (▲) and **3** (■) in 5 mM Tris–HCl buffer medium at 37 ± 0.1 °C.

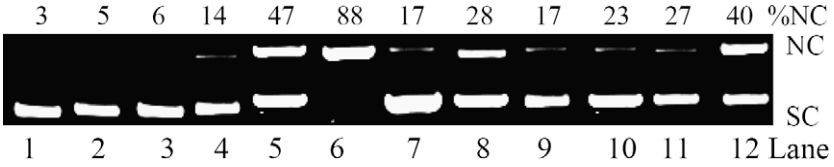

Fig. 7. Gel electrophoresis diagram showing the cleavage of SC pUC19 DNA (0.2 μg, 30 μM) by complexes **1**–**3** (5 μM) in 50 mM Tris–HCl/50 mM NaCl buffer (pH 7.2) in the presence of MPA (0.5 mM): lane 1, DNA control; lane 2, DNA + MPA; lane 3, DNA + **2**; lane 4, DNA + **1** + MPA; lane 5, DNA + **2** + MPA; lane 6, DNA + **3** + MPA; lane 7, DNA + distamycin (10 μM) + **2** + MPA; lane 8, DNA + distamycin (10 μM) + **3** + MPA. lane 9, DNA + DMSO (4 μL) + **2** + MPA; lane 10, DNA + catalase (4 U) + **2** + MPA; lane 11, DNA + KI (10 μM) + **2** + MPA; lane 12, DNA + SOD (4 U) + **2** + MPA.

plexes with DNA. The double-stranded DNA tends to gradually dissociate to single strands on increase in the solution temperature and generates a hyperchromic effect on the absorption spectra of DNA bases (λ_{max} = 260 nm). In order to identify this transition process, the melting temperature T_m, which is defined as the temperature where half of the total base pairs gets non-bonded, is a valuable parameter. Strong intercalation of compounds to DNA generally results in a considerable increase in the melting temperature (T_m) [58]. The DNA melting studies with the present complexes show a moderate positive shift in the melting temperature (ΔT_m) of ~3 °C suggesting primarily electrostatic and/or groove binding nature of the complexes in preference to an intercalative mode of binding to DNA (Fig. 6a, Table 2) [59].

To understand the nature of the interaction between the ternary copper(II) complexes and DNA, viscosity measurements were done. Viscosity parameter is important as it is sensitive to the change in length of the DNA strands and provides valuable information for any conformational change [60]. A strong intercalation of the complex leads to lengthening of DNA helix as base pairs are separated to accommodate the binding ligand, leading to an increase in viscosity of the DNA solution. In contrast, groove binding or partial intercalation leads to only minor changes in the viscosity. Plot of relative specific viscosity $(\eta/\eta_0)^{1/3}$ versus [complex]/[DNA] ratio shows moderate change in the viscosity for the present complexes (Fig. 6b). The results indicate electrostatic and/or groove binding nature of the bpy and phen complexes, and partial intercalative nature of the dpq complex [61].

3.4. DNA cleavage properties

3.4.1. Chemical nuclease activity

The oxidative cleavage of supercoiled (SC) pUC19 DNA (0.2 μg, 30 μM) in 50 mM Tris–HCl/50 mM NaCl buffer (pH, 7.2) by the copper(II) complexes (5 μM) in the presence of a reducing agent (3-mercaptopropionic acid (MPA), 0.5 mM) has been studied by gel electrophoresis (Fig. 7). The DNA cleavage activity follows the order: **3** (dpq) > **2** (phen) ≫ **1** (bpy). Control experiments using MPA or the ternary complexes alone do not show any apparent cleavage of SC-DNA. The bpy complex **1** is cleavage inactive due to its inability to bind to DNA. To determine the groove selectivity of the complexes, control experiments are performed using minor groove binder distamycin. Addition of distamycin significantly inhibits the DNA cleavage by the phen and dpq complexes suggesting their minor groove binding preference. Control experiments show that the hydroxyl radical scavenger catalase or DMSO inhibits the DNA cleavage indicating formation of hydroxyl radical and/or "copper-oxo" intermediate as the reactive species [62,63]. SOD addition does not have any apparent effect on the cleavage activity indicating the non-involvement of O_2^- in the cleavage reaction (Fig. 7). The mechanism involved in the DNA cleavage reactions could be similar to that proposed by Sigman and coworkers for the "chemical nuclease" activity of bis(phen)copper species [1,62,63].

3.4.2. DNA photocleavage activity

Photo-induced DNA cleavage experiments have been carried out in UV-A and visible light using complexes **1**–**3** (5 and 10 μM) and SC pUC19 DNA (0.2 μg, 30 μM) in absence of any external

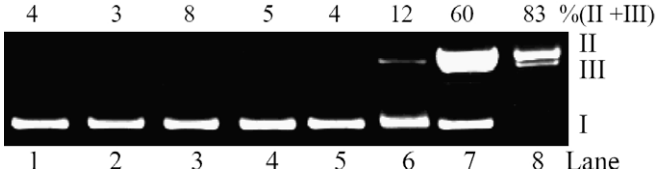

Fig. 8. Gel electrophoresis diagram showing the photo-induced oxidative cleavage of SC pUC19 DNA (0.2 μg, 30 μM) by complexes **1**–**3** (5 μM) in 50 mM Tris–HCl/NaCl buffer (pH 7.2) on irradiation with UV light of 365 nm wavelength: lane 1, DNA control; lane 2, DNA + **3** (dark); lane 3, DNA + dpq (5 μM); lane 4, DNA + L-gln (5 μM); lane 5, DNA + $CuCl_2 \cdot 2H_2O$ (5 μM); lane 6, DNA + **1**; lane 7, DNA + **2**; lane 8, DNA + **3**.

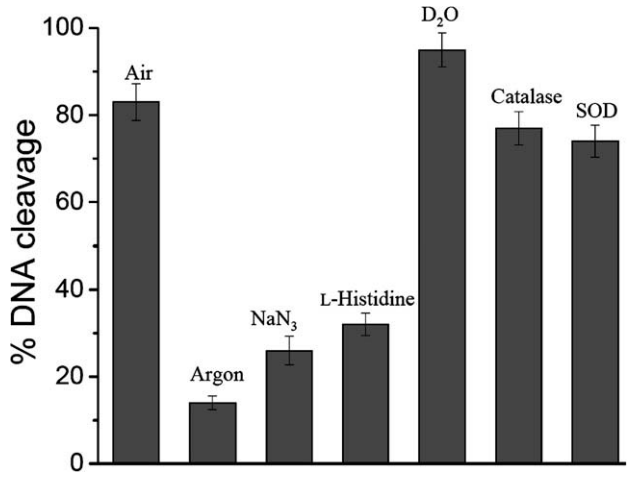

Fig. 9. Bar diagram showing the cleavage of SC pUC19 DNA (0.2 μg, 30 μM) by **3** (10 μM) in the presence of different additives on photo-irradiation at 365 nm for 1 h exposure time in 50 mM Tris–Cl/NaCl buffer (pH 7.2). The additives used are as follows: NaN_3, 10 μM; L-histidine, 10 μM; D_2O, 16 μL; DMSO, 2 μL; catalase, 4 units; SOD, 4 units.

Table 5
Selected cleavage data of SC pUC19 (0.2 μg, 30 μM NP) by complexes **1**–**3**[a]

Sl. no.	Reaction condition	[Complex][a]/μM	%SC	%NC
Chemical nuclease activity in dark				
1	DNA + **2** (dark)	5	94	6
2	DNA + **1** + MPA	5	92	8
3	DNA + **2** + MPA	5	53	47
4	DNA + **3** + MPA	5	12	88
Light source: UV-A light (365 nm, 12 W)				
5	DNA control		96	4
6	DNA + L-gln (10 μM)		95	5
7	DNA + dpq (10 μM)		92	8
8	DNA + **1**	10	90	10
9	DNA + **2**	10	40	60
10	DNA + **3**	10	17	83[b]
Light source: visible light (647.1 nm CW laser, 100 mW)				
11	DNA control		96	4
12	DNA + L-gln (10 μM)		93	7
13	DNA + dpq (10 μM)		91	9
14	DNA + **1**	10	93	7
15	DNA + **2**	10	74	26
16	DNA + **3**	10	14	86[c]

[a] SC and NC are supercoiled and nicked circular forms of DNA, respectively. Exposure time is 1 h in UV-A and visible light. [MPA] = 5 mM.
[b] Contains ~24% linear form of DNA.
[c] Contains ~12% linear form of DNA.

reagent. Complexes 2 and 3 show DNA cleavage activity on photo-exposure to UV-A light of 365 nm and red light of 647.1 nm (Figs. 8–10, Table 5). The bpy complex **1** does not exhibit any photo-induced DNA cleavage activity. Control experiments using complex **2** under dark condition or the amino acid (L-gln) alone do not show any apparent cleavage of the SC DNA at 365 nm. The cleavage efficiency follows the order: **3** > **2** ≫ **1.** The dpq complex **3** shows enhanced photocleavage activity with the formation of both nicked-circular DNA and biologically important linear DNA, while its phen analogue **2** shows formation of only NC form. This could be due to better DNA binding ability of complex **3**, the photosensitization ability of the quinoxaline moiety involving the photoexcited $^3(n–\pi^*)$ or $^3(\pi–\pi^*)$ state(s) and photosensitization of the pendant amide moiety of the amino acid [64]. The phen ligand in metal-bound form is photo inactive. The bis(phen)copper(II) complex does not show any apparent DNA cleavage activity on photo-irradiation at 365 nm. The observed photoactivity of the phen complex **2** could be from photosensitization of the pendant carboxamide group of the amino acid. The photoactivity of the $–CONH_2$ group of L-gln is less than L-lysine and L-arginine having cationic amine and guanidinium pendant groups in their ternary structures [36–38]. The photoactivity of L-methionine with a pendant thiomethyl group in ternary copper(II) complexes is poor as sulfur is susceptible to oxidation by singlet oxygen [35].

The mechanistic aspects of the DNA cleavage reactions have been investigated in UV-A light of 365 nm from various control experiments. Addition of singlet oxygen quencher like sodium azide or histidine inhibits the photocleavage of SC DNA. An enhancement of photocleavage of DNA is observed in D_2O solvent in which singlet oxygen ($^1O_2$) has longer lifetime than in H_2O [65]. Hydroxyl radical scavengers DMSO and catalase do not show any significant inhibition in the DNA cleavage activity. Mechanistic data suggest the formation of singlet oxygen ($^1O_2$) as the reactive species in a type-II process in the metal assisted photo-excitation process involving ligand $n–\pi^*$ and $\pi–\pi^*$ transitions (Fig. 9).

The photo-induced DNA cleavage activity of complexes **2** and **3** (10 μM) has been explored in red light of 647.1 nm using a CW Ar-Kr laser source considering that the PDT drug Photofrin® is active near this wavelength [16,17]. The ligands alone are cleavage inactive at this wavelength. Complex **2** shows only moderate cleavage of DNA from its SC to NC form indicating relatively poor photosensitization ability of the pendant amido group of the amino acid in comparison to the quinoxaline moiety of dpq ligand (Fig. 10, Table 5). The extent of DNA cleavage by the dpq complex **3** is significantly higher than the phen analogue. This is possibly due to enhanced photosensitizing ability of the quinoxaline moiety of the dpq ligand. As the ligands alone are inactive in cleaving DNA at this wavelength, photo-excitation of the complexes seems to be metal-assisted and involves the metal-based d–d transition resulting an excited state that presumably activates oxygen from its stable triplet (O_2, $^3\Sigma_g^-$) to the toxic singlet (O_2, $^1\Delta_g$) state [66,67].

4. Conclusions

In summary, new ternary copper(II) complexes having L-glutamine and heterocyclic bases in a CuN_3O_2 coordination geometry are prepared and structurally characterized by X-ray crystallography. The crystal structures of the complexes show square pyramidal (4+1) coordination geometry in which the amino acid and heterocyclic bases bind at the basal positions. The phen and dpq

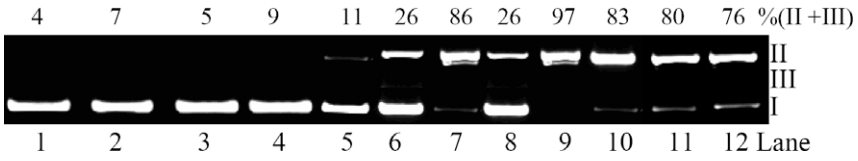

Fig. 10. Red light-induced cleavage of SC pUC19 DNA (0.2 μg, 30 μM) by complexes **1**–**3** (10 μM) in 50 mM Tris–HCl/NaCl buffer (pH 7.2) using a 647.1 nm Ar-Kr CW laser (100 mW) for 1 h exposure time: lane 1, DNA control; lane 2, DNA + L-gln (10 μM); lane 3, DNA + $CuCl_2 \cdot 2H_2O$ (50 μM); lane 4, DNA + dpq (10 μM); lane 5, DNA + **1**; lane 6, DNA + **2**; lane 7, DNA + **3**, lane 8, DNA + **3** + NaN_3, lane 9, DNA + **3** + D_2O (16 μL); lane 10, DNA + DMSO + **3**; lane 11, DNA + catalase (4 U) + **3**; lane 12, DNA + SOD (4 U) + **3**.

complexes display DNA groove binding affinity and show efficient "chemical nuclease" activity in the presence of MPA. The dpq complex shows efficient photo-induced DNA cleavage activity on irradiation with UV-A and red light by a pathway involving the formation of singlet oxygen. The {(L-gln)-Cu(II)} moiety with a pendent carboxamide group exhibits moderate photosensitizing effect in the UV-A light, while planar heterocyclic dipyridoquinoxaline base shows efficient DNA binding and photosensitizing abilities. The $3d^9$-copper(II) plays an important role in assisting the photosensitization process thus making the complexes as model photonucleases in red light within PDT window. The results are of importance as 3d-metal complexes having bio-essential constituents like copper and photoactive α-amino acid showing red light-induced DNA cleavage activity have the potential for designing and developing complexes for cellular applications in photodynamic therapy.

Acknowledgements

We thank the Department of Science and Technology (DST) [SR/S1/IC-10/2004], Government of India, for financial support and the CCD diffractometer facility. A.K.P. and S.R. are thankful to CSIR for fellowship. We also thank the Alexander von Humboldt Foundation, Germany, for donation of an electroanalytical system.

Appendix A. Supplementary material

CCDC 680109, 680110 and 680111 contain the supplementary crystallographic data for **1**, **2** and **3**. These data can be obtained free of charge from The Cambridge Crystallographic Data Centre via www.ccdc.cam.ac.uk/data_request/cif. Unit cell packing diagrams of the crystal structures of **1**–**3** (Figs. S1–S3) are also available. Supplementary data associated with this article can be found, in the online version, at doi:10.1016/j.ica.2008.08.003.

References

[1] D.S. Sigman, Acc. Chem. Res. 19 (1986) 180.
[2] D.S. Sigman, A. Mazumder, D.M. Perrin, Chem. Rev. 93 (1993) 2295.
[3] S.J. Lippard, Chem. Rev. 99 (1999) 2467.
[4] S. van Zutphen, J. Reedijk, Coord. Chem. Rev. 249 (2005) 2845.
[5] J.K. Barton, Science 233 (1986) 727.
[6] K.E. Erkkila, D.T. Odom, J.K. Barton, Chem. Rev. 99 (1999) 2777.
[7] H.T. Chifotides, K.R. Dunbar, Acc. Chem. Res. 38 (2005) 146.
[8] W.K. Pogozelski, T.D. Tullius, Chem. Rev. 98 (1998) 1089.
[9] C.J. Burrows, J.G. Muller, Chem. Rev. 98 (1998) 1109.
[10] D.R. McMillin, K.M. McNett, Chem. Rev. 98 (1998) 1201.
[11] B. Meunier, Chem. Rev. 92 (1992) 1411.
[12] J.A. Cowan, Chem. Rev. 98 (1998) 1067.
[13] E.L. Hegg, J.N. Brustyn, Coord. Chem. Rev. 173 (1998) 133.
[14] L.J.K. Boerner, J.M. Zaleski, Curr. Opin. Chem. Biol. 9 (2005) 135.
[15] T.A. van den Berg, B.L. Feringa, G. Roelfes, Chem. Commun. (2007) 180.
[16] R. Bonnett, Chemical Aspects of Photodynamic Therapy, Gordon & Breach, London, UK, 2000.
[17] M.R. Detty, S.L. Gibson, S.J. Wagner, J. Med. Chem. 47 (2004) 3897.
[18] B.W. Henderson, T.M. Busch, L.A. Vaughan, N.P. Frawley, D. Babich, T.A. Sosa, J.D. Zollo, A.S. Dee, M.T. Cooper, D.A. Bellnier, W.R. Greco, A.R. Oseroff, Cancer Res. 60 (2000) 525.
[19] M. Kar, A. Basak, Chem. Rev. 107 (2007) 2861.
[20] S. Atilgan, Z. Ekmekci, A.L. Dogan, D. Guc, E.U. Akkaya, Chem. Commun. (2006) 4398.
[21] A.M. Angeles-Boza, P.M. Bradley, P.K.-L. Fu, M. Shatruk, M.G. Hilfiger, K.R. Dunbar, C. Turro, Inorg. Chem. 44 (2005) 7262.
[22] J. Brunner, J.K. Barton, J. Am. Chem. Soc. 128 (2006) 6772.
[23] A.A. Holder, D.F. Zigler, M.T. Tarrago-Trani, B. Storrie, K.J. Brewer, Inorg. Chem. 46 (2007) 4760.
[24] A. Sitlani, E.C. Long, A.M. Pyle, J.K. Barton, J. Am. Chem. Soc. 114 (1992) 2303.
[25] T.K. Janaratne, A. Yadav, F. Ongeri, F.M. MacDonnell, Inorg. Chem. 46 (2007) 3420.
[26] F.S. Mackay, J.A. Woods, P. Heringová, J. Kašpárková, A.M. Pizarro, S.A. Moggach, S. Parsons, V. Brabec, P.J. Sadler, Proc. Natl. Acad. Sci. USA 104 (2007) 20743.
[27] P.J. Benites, R.C. Holmberg, D.S. Rawat, B.J. Kraft, L.J. Klein, D.G. Peters, H.H. Thorp, J.M. Zaleski, J. Am. Chem. Soc. 125 (2003) 6434.
[28] S. Dhar, D. Senapati, P.K. Das, P. Chattopadhyay, M. Nethaji, A.R. Chakravarty, J. Am. Chem. Soc. 125 (2003) 12118.
[29] P.K. Sasmal, A.K. Patra, M. Nethaji, A.R. Chakravarty, Inorg. Chem. 46 (2007) 11112.
[30] M. Roy, S. Saha, A.K. Patra, M. Nethaji, A.R. Chakravarty, Inorg. Chem. 46 (2007) 4368.
[31] M. Roy, B. Pathak, A.K. Patra, E.D. Jemmis, M. Nethaji, A.R. Chakravarty, Inorg. Chem. 46 (2007) 11122.
[32] M.-J. Fernández, B. Wilson, M. Palacios, M.-M. Rodrigo, K.B. Grant, A. Lorente, Bioconjugate Chem. 18 (2007) 121.
[33] T.D. Maurer, B.J. Kraft, S.M. Lato, A.D. Ellington, J.M. Zaleski, Chem. Commun. (2000) 69.
[34] A.K. Patra, S. Dhar, M. Nethaji, A.R. Chakravarty, Chem. Commun. (2003) 1562.
[35] A.K. Patra, S. Dhar, M. Nethaji, A.R. Chakravarty, Dalton Trans. (2005) 896.
[36] A.K. Patra, M. Nethaji, A.R. Chakravarty, Dalton Trans. (2005) 2798.
[37] A.K. Patra, M. Nethaji, A.R. Chakravarty, J. Inorg. Biochem. 101 (2007) 233.
[38] A.K. Patra, T. Bhowmick, S. Ramakumar, A.R. Chakravarty, Inorg. Chem. 46 (2007) 9030.
[39] K.P. Mahon Jr., R.F. Ortiz-Meoz, E.G. Prestwich, S.O. Kelly, Chem. Commun. (2003) 1956.
[40] L.M. Wittenhagen, J.R. Carreon, E.G. Prestwich, S.O. Kelley, Angew. Chem., Int. Ed. 44 (2005) 2542.
[41] B. Breiner, J.C. Schlatterer, S.V. Kovalenko, N.L. Greenbaum, I.V. Alabugin, Angew. Chem., Int. Ed. 45 (2006) 3666.
[42] D.D. Perrin, W.L.F. Armarego, D.R. Perrin, Purification of Laboratory Chemicals, Pergamon Press, Oxford, 1980.
[43] J.G. Collins, A.D. Sleeman, J.R. Aldrich-Wright, I. Greguric, T.W. Hambley, Inorg. Chem. 37 (1998) 3133.
[44] O. Khan, Molecular Magnetism, VCH, Weinheim, 1993.
[45] N. Walker, D. Stuart, Acta Crystallogr., Sect. A 39 (1983) 158.
[46] G.M. Sheldrick, SHELX-97, Program for Crystal Structure Solution and Refinement, University of Göttingen, Göttingen, Germany, 1997.
[47] C.K. Johnson, ORTEP-III, Report ORNL – 5138, Oak Ridge National Laboratory, Oak Ridge, TN, 1976.
[48] J. Marmur, J. Mol. Biol. 3 (1961) 208.
[49] M.E. Reichmann, S.A. Rice, C.A. Thomas, P. Doty, J. Am. Chem. Soc. 76 (1954) 3047.
[50] J.D. McGhee, P.H. von Hippel, J. Mol. Biol. 86 (1974) 469.
[51] M.T. Carter, M. Rodriguez, A.J. Bard, J. Am. Chem. Soc. 111 (1989) 8901.
[52] M.J. Waring, J. Mol. Biol. 13 (1965) 269.
[53] J.-B. LePecq, C. Paoletti, J. Mol. Biol. 27 (1967) 87.
[54] M. Lee, A.L. Rhodes, M.D. Wyatt, S. Forrow, J.A. Hartley, Biochemistry 32 (1993) 4237.
[55] J. Bernadou, G. Pratviel, F. Bennis, M. Girardet, B. Meunier, Biochemistry 28 (1989) 7268.
[56] A.W. Addison, T.N. Rao, J.V. Reedijk, G.C. Verschoor, J. Chem. Soc., Dalton Trans. (1984) 1349.
[57] J.K. Barton, A.T. Danishefsky, J.M. Goldberg, J. Am. Chem. Soc. 106 (1984) 2172.
[58] L.E. Gunther, A.S. Yong, J. Am. Chem. Soc. 90 (1968) 7323.
[59] Y. An, S.-D. Liu, S.-Y. Deng, L.-N. Ji, Z.-W. Mao, J. Inorg. Biochem. 100 (2006) 1586.
[60] G. Cohen, H. Eisenberg, Biopolymers 8 (1969) 45.
[61] S. Satyanarayana, J.C. Dabroniak, J.B. Chaires, Biochemistry 32 (1993) 2573.
[62] O. Zelenko, J. Gallagher, D.S. Sigman, Angew. Chem., Int. Ed. Engl. 36 (1997) 2776.
[63] T.B. Thederahn, M.D. Kuwabara, T.A. Larsen, D.S. Sigman, J. Am. Chem. Soc. 111 (1989) 4941.
[64] K. Toshima, R. Takano, T. Ozawa, S. Matsumura, Chem. Commun. (2002) 212.
[65] A.U. Khan, J. Phys. Chem. 80 (1976) 2219.
[66] K. Szacilowski, W. Macyk, A. Drzewiecka-Matuszek, M. Brindell, G. Stochel, Chem. Rev. 105 (2005) 2647.
[67] B. Armitage, Chem. Rev. 98 (1998) 1171.